A Ray-Tracing Method for Predicting Delay Spread in Tunnel Environments

Mohammad Haeri Kermani, and Mahmuoud Kamarei
Department of Electrical and Computer Eng., University of Tehran, Tehran, Iran
Phone: +98-21-8778690
E-mail: mayan@www.dci.co.ir

ABSTRACT

Our model to predict the propagation is based on ray-tracing which uses images algorithm to find paths between transmitter and receiver. It accounts for all rays reach the receiver location after an arbitrary number of reflections and includes the effect of the angle of incidence, the material dielectric constant, the antenna pattern and polarization, the wall roughness, and the tunnel cross section size. The simulation results in this paper are obtained by analyzing much less rays compared to the other published results. The results illustrate that in an empty straight rectangular tunnel environment, propagation has a very short time delay spread. Meanwhile, the results have shown that rms delay spread for horizontally polarized transmit and receive antennas is more than vertically polarized transmit and receive antennas, in which the attenuation constant is less when transmit and receive antennas are horizontally polarized than when they are vertically polarized. Finally, by using a specific pattern, the rms delay spread has decreased compared to an isotropic antenna.

INTRODUCTION

The ability to predict delay spread is crucial for planning interference reduction strategies in wireless radio system design. The characteristic parameters of an outdoors mobile radio channel are different compared to those of the tunnel environment radio channel. Therefore, the characteristic parameters of tunnel environment radio channel should be determined by separate series of research.

In view of the large tunnel dimensions relative to the free space wavelength, a geometrical ray approach is used to evaluate narrow-band and wide-band propagation characteristics [3,6]. Narrow-band is characterized in terms of attenuation constant. The attenuation constant versus distance in a straight rectangular tunnel environment is calculated in [1].

The characteristics of wide-band radio propagation channels can be roughly quantified by the rms delay spread τ_{rms}, defined as:

$$\tau_{rms} = \sqrt{\frac{\sum_k (t_k - \tau_m)^2 a_k^2}{\sum_k a_k^2}} \quad (1)$$

Where:

$$\bar{\tau} = \frac{\sum_k t_k a_k^2}{\sum_k a_k^2} \quad (2)$$

is the mean excess delay and the time axis is scaled such that the first path in a profile arrives at $t_1 = 0$.

The above expressions show that τ_m is the first moment of the power delay profile with respect to the first arriving path, and the rms delay spread τ_{rms} is the square root of the second central moment of a power delay profile. Performance of digital communication systems operating in multipath environments is very sensitive to the value of τ_{rms}. Recent studies have shown that in order to have a tolerable ISI[1], the ratio of rms delay spread to symbol duration must be kept below 0.2 for digital communication systems with no diversity or equalization [2]. Therefore, precise analysis of τ_{rms} can provide valuable information for digital communication systems design.

RAY-TRACING METHOD BASED ON IMAGES ALGORITHM

Ray-tracing method is based on electromagnetic-wave propagation theory to characterize indoor propagation. It uses geometrical ray approach to obtain the fields at any point in the environment as a summation of rays from all possible paths, avoiding the elaborate task of determining the modal propagation constants. This method is applicable when the environment dimensions are somewhat greater than a free-space wavelength, which is mostly true in tunnel applications.

Ray-tracing is most accurate when the point of observation is many wavelengths from the nearest scatters, all scatters

[1] Intersymbol interference

0-7803-5893-7/00/$10.00 © 2000 IEEE

are large compared to a wavelength, and smooth, i.e. have surface features that are small compared to a wavelength. Hence, only objects that are much larger than a free-space wavelength should be considered in database.

Three main areas of error in a ray-tracing method are propagation modeling errors, database errors, and kinematic errors. Propagation modeling errors come from the geometrical optics models used to describe radio wave behavior. Database errors stem from the limitations of a finite, numerical description of the world. Therefore, in order to obtain an accurate prediction of signal propagation inside a building, a greater detail of the indoor environment is required. The ability of a ray-tracing algorithm to find and interpret radiation paths determines the kinematic errors of a simulation.

Finding the paths between transmitter and receiver is a demanding job in ray-tracing method. There are two algorithms –the images algorithm [6] and brute force ray tracing algorithm- to find paths between transmitter and receiver. For scatters bounded by plane faces it is convenient to employ the images algorithm. This algorithm is well suited to radio propagation analysis in the case of geometry of low complexity and where a low number of reflections are considered. The images algorithm uses image theory to place artificial sources in the environment that model reflections from the flat planes of a database. Because images algorithm determines exact radiation paths, the images algorithm introduces no errors into the radiation paths it finds. However, this algorithm is only valid for reflected modes of propagation, since diffraction introduces indefinite degrees of freedom in the direction of a ray path.

This algorithm assumes every plane face in an indoor environment to be a mirror. For line-of-sight propagation, it is easy to trace the ray by connecting the transmitter and receiver. For single-reflection propagation, the radio source is mirrored at a particular face. The point of intersection of the mirror face and the line connecting the transmitter image to the receiver is the point where specular reflection occurs. The single-reflection propagation path can then be obtained by connecting the source point, reflection point and receiver point. For repeated reflection, the image of the radio source with reference to a particular plane face is found first. The next step is to find an image of the source image with reference to another plane face where the second point of reflection will be located. Following the same rule, all the points of reflection at the relevant plane faces can be obtained and then the multiple-reflection propagation paths can be obtained. The algorithm described above, starting at the source image, is referred to as the forward ray-tracing method. It is also possible to begin with at the receiver image and trace back to the transmitter. This is called the backward ray-tracing method [6].

The primary drawback to images algorithm is its heavy dependence on the number of elements in the environment database. For single reflection, each additional surface in the database can double the number of images available to a receiver. Therefore, images algorithm should not be used to render complicated, three-dimensional structures, which require multiple reflections from hundreds of surface.

After finding the paths between transmitter and receiver, the received power should be calculated. The received power is mathematically expressed in general as:

$$P_r = P_t\left\{\frac{\lambda}{4\pi}\right\}^2\left\{\left|\frac{G_d(x)}{r}+\sum_{i=1}^{N-1}\frac{G_{R_i}(x)R_i\exp(j\varphi_i)}{r_i}\right|^2\right\} \tag{3}$$

in which the parameters are defined as follows:

P_r : Received power

P_t : Transmitted power

λ : Free-space wavelength

G_d : The square root of the multiplication of the transmit antenna gain and receive antenna gain in LOS direction

G_{r_i} : The square root of the multiplication of the transmit antenna gain in the direction of its launched *i*th ray and receive antenna gain in the direction of its received *i*th ray.

r : Path length of line-of-sight

r_i : Path length of *i*th ray

R_i : Reflection coefficient of the *i*th ray undergone some specular reflections from corresponding reflected surfaces and then intercepted by the receive antenna. If the surface is not smooth, the reflection coefficient should be corrected as follows:

$$(R_i)_{rough} = \rho_s R_i \tag{4}$$

in which scattering loss factor (ρ_s) is defined as:

$$\rho_s = \exp\left[-8\left(\frac{\pi\sigma_h\cos(\varphi)}{\lambda}\right)^2\right] \text{[5]} \tag{5}$$

$$\varphi_i = \frac{2\pi\Delta l_i}{\lambda} \tag{6}$$

(Δl_i is the distance difference between line-of-sight and *i*th path)

$$R_{h_i} = \frac{\cos(\varphi_i)-(\varepsilon-\sin^2(\varphi_i))^{\frac{1}{2}}}{\cos(\varphi_i)+(\varepsilon-\sin^2(\varphi_i))^{\frac{1}{2}}} \tag{7}$$

is the reflection coefficient for a ray reflected once from a reflected surface and this ray is horizontally polarized with respect to the surface.

$$R_{v_i} = \frac{\varepsilon\cos(\varphi_i)-(\varepsilon-\sin^2(\varphi_i))^{\frac{1}{2}}}{\varepsilon\cos(\varphi_i)+(\varepsilon-\sin^2(\varphi_i))^{\frac{1}{2}}} \tag{8}$$

is the reflection coefficient for a ray reflected once from reflected surface and this ray is vertically polarized with respect to the surface

In (5) and (6), φ_i represents the angle of incidence for the ray, and $\varepsilon_i = \varepsilon_{r_i} - j60\sigma_i\lambda_i, i = 1,2$ are complex relative dielectric constants of lossy media. ε_{r_i} and σ_i are relative permittivity and conductivity of the media, respectively.

Although the above reflection coefficients are strictly valid only for incident plane waves on infinite plane interface, they are practically as valid for incident spherical waves when these are several wavelength from the source and when the interface is only of finite extent. In other words, the waves emanating from the source are assumed to be sharply defined rays far enough from the source, and hence their reflections are affected only by the local conditions of the interface. This is actually the basis of developing the ray series to follow for the fields in the tunnel where cross-sectional dimensions are sufficiently greater than a free-space wavelength.

The algorithm has been made more realistic by giving both transmitting and receiving antenna gain patterns. The gain of the half-wave dipole is given in the **APPENDIX**.

A computer program has been written to implement the model described in this section as an automated propagation prediction tool.

SIMULATIONS

In this section, we calculate power delay profiles by using the ray-tracing method described in previous section and then analyze wide-band propagation characteristics in tunnel environments.

The geometry of a typical tunnel and chosen coordinate system are shown in Fig. 1 (z direction is along the tunnel). The transmit and receive antennas are assigned to points referenced by three-dimensional coordinates. The tunnel walls are assumed to be a lossy nonmagnetic homogeneous medium with relative permittivity ε_r and conductivity σ

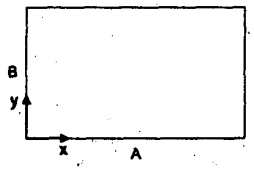

Fig. 1- Geometry of the tunnel.

At first, in order to assess the validity of the simulation results, comparisons were made with measurements carried out inside a tunnel and published by [3]. Fig. 2 shows the simulated results in an empty straight tunnel with a rectangular cross section 4m high and 7.5m wide. Curve (1) shows the measured result of the variation of the received signal power level versus the distance between the transmitter and the receiver at 900MHz. The transmit and receive antennas are half-wave length dipoles, vertically polarized and located at (0.25A, 0.3B, z_0) and (0.2A, 0.3B, z), respectively (A is the width of the tunnel, and B is the height of the tunnel). Curve (2) represents the simulated received power from the propagation model used in that paper with the electrical characteristics of the tunnel walls being $\varepsilon_r = 10$ and $\sigma = 10^{-2} s/m$ which has been vertically displaced from curve (1) for better comparison.

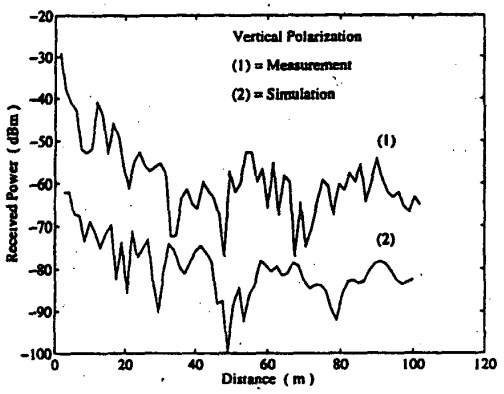

Fig. 2- Measured and simulated received power at 900MHz in an empty straight rectangular tunnel (the simulated one is displaced 30dB downward) [3].

Fig. 3 is a plot of the simulated received power from the propagation model used in this paper in the longitudinal direction, against the distance between transmitter and receiver. The longitudinal spatial patterns of the predicted and measured values are quite similar and follow the same trend. Therefore, our propagation model is an efficient model for predicting propagation. However, the predicted values consistently underestimate the measured propagation loss. This may well be due to the fact that, so far, we have assumed lowless dielectric layers at the reflection points and roughness factor is not precisely determined. Also, since the walls are modeled as homogeneous structures, the scattering due to the inhomogeneous composite materials can cause significant modeling errors in phase and magnitude. Clearly, some adjustments is to be made to account for scattering losses due to surface roughness, and the effective complex dielectric constants used for the walls.

Curves (1) and (2) in Fig. 4 illustrate the predicted results of the variation of the received signal power levels versus the distance between the transmitter and the receiver at 900MHz for horizontal and vertical polarization, respectively. The attenuation constant is determined in the conventional manner by applying regression analysis to the received signal data file. The results are summarized in table 1. It is found that horizontally polarized signals have smaller attenuation constant than vertically polarized ones. Note that the measured attenuation constants are also different from

that predicted by tunnel imperfect waveguide theory. The attenuation constant was determined to be one presented in [1] in which only the fundamental mode was considered. Predicted data observed that the contribution of the signal not only from the fundamental mode, but also from other significant higher order ones.

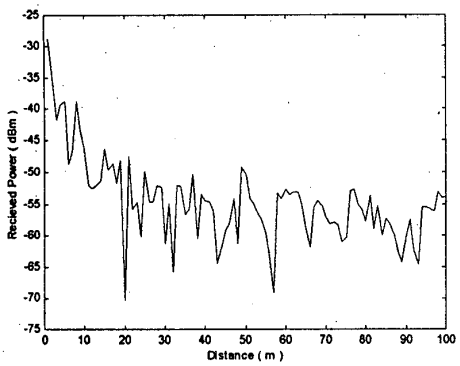

Fig. 3- Simulated received power at 900MHz in an empty straight rectangular tunnel for vertically polarized transmit and receive antennas.

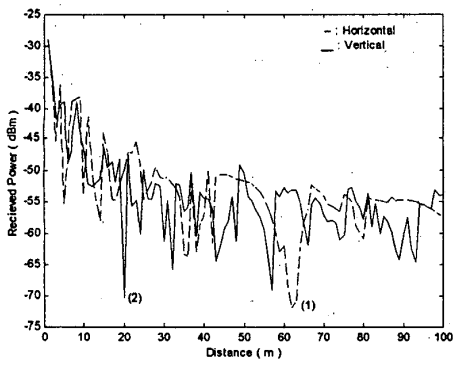

Fig. 4- Simulated received power at 900MHz in an empty straight rectangular tunnel for vertically and horizontally polarized transmit and receive antennas.

The wide-band comparison was made in temporal domain. Figs. 5 and 6 display the 900MHz predicted power delay profiles for horizontal and vertical polarization with 10-m separation between the transmit and receive antennas, respectively. The amplitude and arrival times of direct path and significant multipath components are correctly predicted. The arrival time of direct wave with the longest amplitude is shown at 33.33ns. The time-of-arrival of the direct wave is estimated from the length of the shortest propagation path.

The horizontally polarized power delay profiles spread somewhat wider than the vertically polarized ones. For example, the simulated rms delay spread for the profile shown in Fig. 5 was 6.79ns for horizontal polarization and decreased to 3.70ns for vertical polarization. More significant echoes for horizontal polarization than those for vertical polarization are observed, since the attenuation for the horizontally polarized wave is smaller than that of the vertically polarized mode.

Table 1- The attenuation constants calculated from theoretical relation in [1] and simulated received power.

	Polarization	Attenuation constant (dB/m)
Theoretical relation [1]	Horizontal	0.0063
Simulation	Horizontal	0.0147
Theoretical relation [1]	Vertical	0.0255
Simulation	Vertical	0.0214

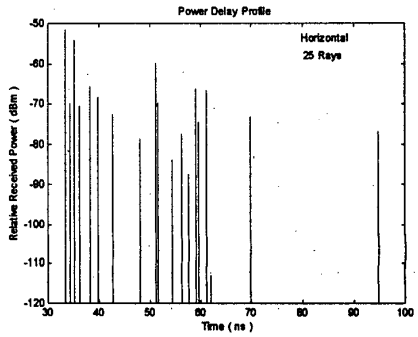

Fig. 5- Simulated power delay profile at 900MHZ in an empty straight rectangular tunnel for horizontal polarization.

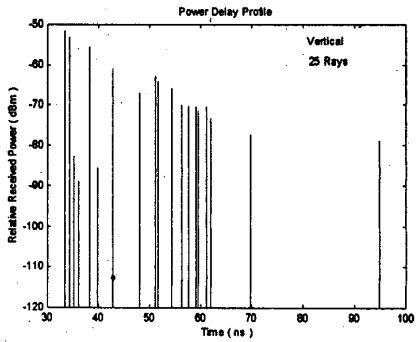

Fig. 6- Simulated power delay profile at 900MHZ in an empty straight rectangular tunnel for vertical polarization.

Fig. 7 shows the simulation results when the tunnel walls are not smooth ($\sigma_h = 10cm$). It illustrates that received power for rough surface is less than smooth surface.
By using the optimum pattern for increasing the area of coverage ($\sin^3(\theta)$) obtained in [4], the rms delay spread has decreased to 3.14ns, in which it was 3.70ns for an isotropic antenna.

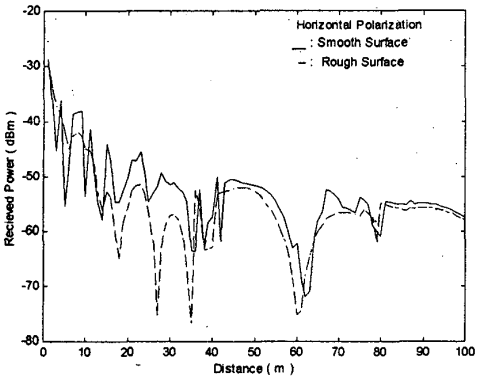

Fig. 7- Simulated received power at 900MHz in an empty straight rectangular tunnel with $\sigma_h = 0$ and $\sigma_h = 10cm$.

SUMMARY AND CONCLUSION

We have described an efficient three-dimensional ray-tracing method, which incorporates images algorithm for finding the paths between transmitter and receiver. Our model accounts for all rays reach the receiver location after an arbitrary number of reflections. This model includes the effect of the angle of incidence, the material dielectric constant, the antenna polarization, the antenna location, the antenna pattern, the wall roughness, and the tunnel cross section size.
To demonstrate the accuracy of predicted results, at first they have been compared against measurements presented in [3] and then, they have been compared with theoretical relation [1]. Both these comparisons validate our results. Our simulation results have been obtained by analyzing of 52 rays, but the simulation results reported in [3] have been obtained by analyzing of more than 1900 rays. This illustrates that our pathfinding algorithm is optimum for tunnel environment.
Our results illustrate when transmit and receive antennas are horizontally polarized, the attenuation constant is less than when they are vertically polarized, which is in agreement with theoretical relation.
Power delay profiles are calculated for analyzing of wide-band propagation characteristics. The obtained power delay profiles show that amplitudes and time delay of many significant multipath components are accurately predicted. The results illustrate that in an empty straight rectangular tunnel environment, propagation has very short time delay spread and as a result it has a broad coherent bandwidth which imply the possible high data rate transmission without equalization. Meanwhile, the results have illustrated that rms delay spread for horizontally polarized transmit and receive antennas is more than vertically polarized transmit and receive antennas.
Finally, by using the optimum pattern for increasing the area of coverage, the rms delay spread has decreased compared to an isotropic antenna.

APPENDIX

A half-wavelength standard dipole was used for both transmit and receive antennas in the simulation. The gain of the antenna is

$$1.64\left[\frac{\cos\left(\frac{\pi}{2}\cos\theta\right)}{\sin\theta}\right]^2 \qquad \text{(A1)}$$

Where θ is measured from the axis of the dipole.

REFERENCES

[1] A.G. Emslie, R. L. Lagace, and P. F. Strong, "Theory of the propagation of UHF radio waves in coal mine tunnels," *IEEE Transactions on Antennas and Propagation*, Vol. AP-23, No. 2, pp. 192-205, March 1975.
[2] H. Hashemi, and D. Tholl, "Statistical modeling and simulation of the RMS delay spread of indoor radio propagation channels," *IEEE Transactions on Vehicular Technology*, Vol. 43, No. 1, pp. 110-120, Feb. 1994.
[3] Y. P. Zhang, Y. Hwang, and R. G. Kouyoumjian, "Ray-optical prediction of radio-wave propagation characteristics in tunnel environments- part 2: analysis and measurements," *IEEE Transactions on Antennas and Propagation*, Vol. 46, No. 9, pp. 1337-1345, Sep.1998.
[4] K. Fujimori, and H. Arai, "Ray-tracing analysis of propagation characteristics in tunnels including transmitting antenna," in *Proceedings of Antennas and Propagation Society International Symposium*, AP-S, Vol. 2, pp. 1222-1225, 1996.
[5] P. Beckman, and A. Spizziochino, The Scattering of Electromagnetic Waves From Rough Surfaces, Artech, 1987.
[6] R. A. Valenzuela, "A ray-tracing approach to predicting indoor wireless transmission," in *Proceedings of 43rd IEEE Vehicular Technology Conference*, pp. 214-218, 1993.